DOI: 10.1002/chem.201001251

Condensation- and Crystallinity-Controlled Synthesis of Titanium Oxide Films with Assessed Mesopores

Tatsuo Kimura,*[a] Yusuke Yamauchi,[b, c] and Nobuyoshi Miyamoto[d]

Materials with controlled microstructures based on sol–gel science have been widely applied to intelligent adsorbents, catalyst supports, photocatalysts, and ceramics in high-performance electronic, photonic, and magnetic devices. Sol–gel reactions of metal alkoxides, such as hydrolysis and condensation, in general lead to the formation of inorganic oxide networks. Compositional design in the frameworks is possible in mixed alkoxide systems. Non-hydrolytic routes have often facilitated the fabrication of mixed metal oxides[1] and inorganic–organic hybrid materials.[2] Likewise, self-adjusted reactions between appropriate inorganic acidity and alkalinity pairs are a powerful method of constructing not only single and/or mixed metal oxides but also metal phosphates.[3] Although these studies have only focused on the initial formation of inorganic networks, subsequent condensation has not been discussed as adequately. Condensation reactions of transition-metal oxides are too fast and it is still difficult to control microstructures atomically in the final metal oxides. Control of the sol–gel reactions has been investigated further by using chemical modification of metal alkoxides with organic chelating agents; the hydrolysis reaction rates of the hydrophobic metal species are lower than those of the original precursors.[4] However, once the designed alkoxides have been hydrolyzed by the presence of water, it becomes difficult to manage subsequent condensation reactions between the metal species, which is a limitation of using sol–gel chemistry with highly reactive transition-metal chlorides and alkoxides.

Herein we demonstrate an effective way for preventing from continuous condensation of transition-metal species in solution by the addition of phosphites. For example, we have found that triethyl phosphite ($P(OC_2H_5)_3$) hardly reacts with transition-metal sources such as $TiCl_4$, $ZrCl_4$, and $FeCl_3$ in ethanol, and unreacted $P(OC_2H_5)_3$ can be eliminated by evaporation under ambient conditions even after the fabrication of the precursor solutions. Accordingly, the poor reactivity of $P(OC_2H_5)_3$ with transition-metal species is utilized for specific control of the degree of condensation in the final inorganic oxides. This protocol is worth investigating to achieve precise control of the condensation reactions between transition-metal species, which should offer advances in the field of sol–gel science. Although it has often been reported that phosphorous sources, such as esters ($OP(OR)_3$, R = alkyl group), acids (H_3PO_4), and chlorides (PCl_3, PCl_5, $OPCl_3$), are generally reactive with proper metal sources, such as alkoxides and salts,[3] the reactivity of $P(OC_2H_5)_3$ has not yet been discussed in the sol–gel science. Condensation-controlled synthesis of surfactant-assisted mesoporous titanium oxide in the presence of $P(OC_2H_5)_3$ was investigated as a typical example because titanium oxide is one of the most intelligent photocatalytic[5,6] and semiconducting[7–9] transition-metal oxides

$TiCl_4$ and $P(OC_2H_5)_3$ were mixed in ethanol (without water) and combined with an ethanolic solution of Pluronic F127 ($EO_{106}PO_{70}EO_{106}$). When $TiCl_4$ was slowly added to an ethanolic solution of $P(OC_2H_5)_3$, it reacted vigorously with ethanol to generate HCl. Because nonhydrolytic reactions between derivative $TiCl_{4-x}(OC_2H_5)_x$ and $P(OC_2H_5)_3$ hardly proceeded in the solution, a resultant precursor solution was

[a] Dr. T. Kimura
Advanced Manufacturing Research Institute
National Institute of Advanced Industrial
Science and Technology (AIST)
Shimoshidami, Moriyama-ku, Nagoya 463-8560 (Japan)
Fax:(+81) 52-736-7234
E-mail: t-kimura@aist.go.jp

[b] Dr. Y. Yamauchi
World Premier International (WPI) Research Center for
Materials Nanoarchitectonics (MANA)
National Institute for Materials Science (NIMS)
Namiki, Tsukuba, Ibaraki 305-0044 (Japan)

[c] Dr. Y. Yamauchi
Precursory Research for Embryonic Science and
Technology (PRESTO) (Japan)
Science and Technology Agency (JST)
Kawaguchi, Saitama 332-0012 (Japan)

[d] Dr. N. Miyamoto
Department of Life, Environment and Materials Science
Fukuoka Institute of Technology, Wajiro-Higashi
Higashi-ku, Fukuoka 811-0295 (Japan)

Supporting information for this article is available on the WWW under http://dx.doi.org/10.1002/chem.201001251.

useful and stable for the fabrication of a cubic $Im\bar{3}m$ mesostructured film in the presence of Pluronic F127 (see the Supporting Information, Figure S1). When a similar synthesis was carried out in the absence of $P(OC_2H_5)_3$, the formation of analogous mesostructured titania film was not observed even in the presence of the triblock copolymer, as observed by X-ray diffration (XRD) and grazing-incidence small-angle X-ray scattering (GI-SAXS; see the Supporting Information, Figure S1). Accordingly, it is thought that the poor reactivity of $P(OC_2H_5)_3$ with transition-metal species plays an important role in preventing condensation reactions between derivative $TiCl_{4-x}(OC_2H_5)_x$ species. Although it has been reported that acetic acid is useful as an organic ligand to stabilize transition-metal species in ethanol,[10] the use of $P(OC_2H_5)_3$ as a non-metallic stabilizer based on inorganic chemistry is rather exceptional and interesting because it is not associated with chemical reactions in precursor solutions and can be recovered for reuse in practical manufacturing process.

A cubic $Im\bar{3}m$ mesostructured film constructed from titanium oxide frameworks without phosphorous species was obtained by spin-coating the precursor solution (a mixture of $TiCl_4$, $P(OC_2H_5)_3$, and Pluronic F127) onto a substrate. The energy-dispersive spectroscopic (EDS) mapping of the as-prepared film (after air-drying and storing in vacuum) showed the presence of only Ti and O atoms across the whole film (see the Supporting Information, Figure S2). Also, the corresponding energy-dispersive X-ray spectroscopic (EDX) spectrum supported the finding that the amount of P atoms present was negligible. The formation mechanism of the titanium oxide-based mesostructured film is illustrated in Scheme 1. The precursor solution was clear and, therefore, both titanium oxo species and $P(OC_2H_5)_3$ should be distributed homogeneously in the film after spin-coating, but $P(OC_2H_5)_3$ was gradually evaporated from the film, even at room temperature, because of its low connectivity to the titanium species. Consequently, a mesostructured film was fabricated from titanium oxide-based frameworks in a less-condensed state. A periodic mesoporous titania film was then obtained after elimination of Pluronic F127 through substantial shrinkage of the frameworks by calcination.

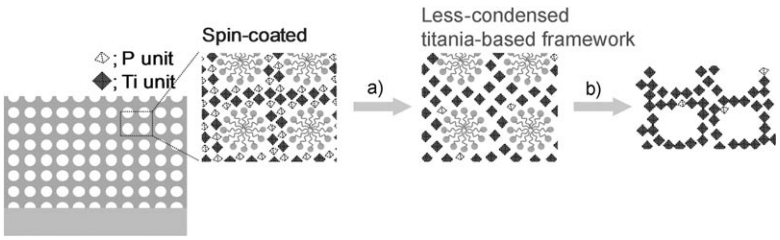

Scheme 1. Schematic formation mechanism of mesostructured precursor film constructed by less-condensed titania-based frameworks in the presence of $P(OC_2H_5)_3$. a) Air-dried to evaporate $P(OC_2H_5)_3$; b) calcined at 250 °C to remove triblock copolymer, resulting in substantial shrinkage.

The less-condensed state of the titania-based frameworks was also confirmed by the GI-SAXS of the as-coated film (see the Supporting Information, Figure S3). The image shows a diffraction pattern with (110), (101) and $(1\bar{1}0)$ peaks that are typically assignable to a deteriorated $Im\bar{3}m$ mesostructure ($d_{1-10}=12.0$ nm, initial $a=17$ nm)[11,12] with the main [110] orientation perpendicular to the substrate.[13] The d_{110} value (8.1 nm) perpendicular to the substrate was shrunk by 47.7 % after drying at room temperature; normally such a substantial shrinkage is not observed even after calcination. Accordingly, the result indicates that the titania-based frameworks are extremely soft due to suppression of condensation reactions in the presence of $P(OC_2H_5)_3$. The transmission electron microscopic (TEM) image of the film calcined at 250 °C shows significant deterioration of the mesostructure, with considerable shrinkage of the less-condensed frameworks (Figure 1).

Variation in the mesostructure during calcination was investigated by using GI-SAXS and TEM (Figure 1). Detailed GI-SAXS data (see the Supporting Information, Figure S3) of films calcined at different temperatures are used to explain the structural variation schematically (see the Supporting Information, Figure S4). The HR-TEM images (see the Supporting Information, Figure S5) showed that the mesostructure was maintained after calcination at 250 °C and seems to be maintained even after calcination at 400 °C. However, it was not transformed into anatase nanopillars, which were observed for the film calcined at 550 °C. Our previous work demonstrated that the $Im\bar{3}m$ mesostructure was almost deformed after calcination at 400 °C, with full crystallization to the titania anatase phase.[14] Here, slight crystallization occurred at 400 °C because the condensation degree of the initial titania-based frameworks is lower than that in the previous study. Therefore, it is important for predicting the mesostructural stability, which is related to the precisely managed degree of condensation of the initial frameworks.

The crystallinity of the calcined films was investigated by using TEM and synchrotron XRD. Crystallization of titania frameworks started at around 400 °C, and after calcination at 550 °C a clear ring pattern assignable to the (101) peak of anatase was confirmed in the fast Fourier transform (FFT) TEM image (see the Supporting Information, Figure S5). Crystallization of titania frameworks was evaluated quantitatively by synchrotron XRD on the basis of the intense (101) peak areas of anatase in the range of $2\theta=25$ to 26° (Figure 2a). Assuming the crystallinity of the titania (anatase) framework to be 1.00 after calcination at 700 °C, the films calcined at 400 and 550 °C are estimated to be 0.56 and 0.58. This result in turn implies that the amorphous phase is

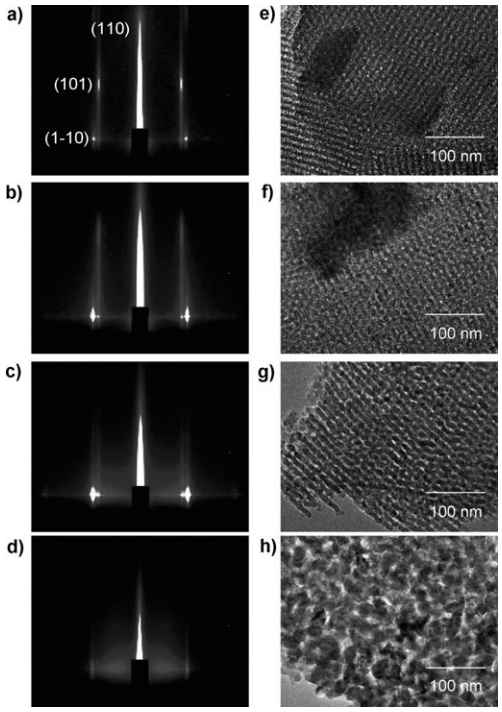

Figure 1. a)–d) GI-SAXS patterns and e)–h) TEM images of Pluronic F127-templated titania-based films calcined at 250 (a,e), 400 (b,f), 550 (c,g), and 700 °C (d,h). The spots next to the $(1\bar{1}0)$ spots are due to the presence of different orientations ([001] perpendicular to the substrate) as a minor component.[13]

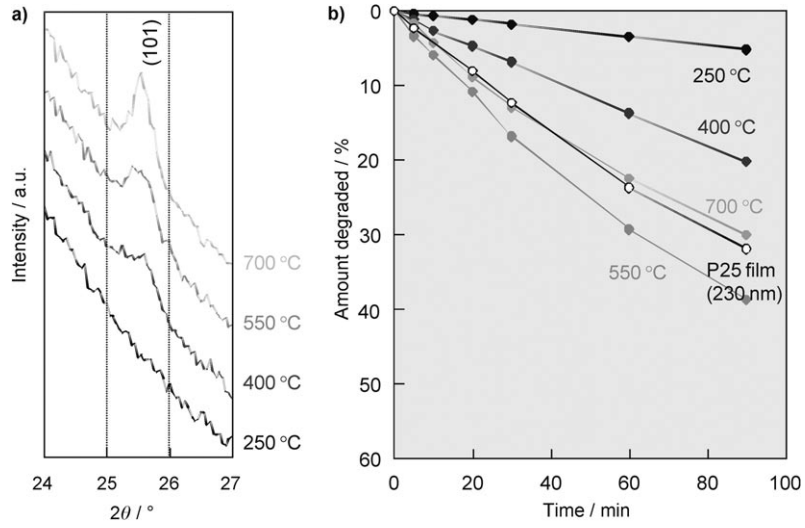

Figure 2. a) Synchrotron XRD patterns of Pluronic F127-templated titanium oxide films calcined at different temperatures and b) the photodegradation of MB at 30 °C under UV irradiation.

actually present even in frameworks calcined at 550 °C. It is considered that the presence of amorphous phase is important for preserving the regularity of the mesostructure and the regular anatase nanopillars because the regularity is finally collapsed by grain growth during calcination at 700 °C, with the formation of intercrystalline mesospaces. There have been many examples of amorphous titania frameworks crystallizing into anatase without the deformation of mesostructures.[11–15] Full crystallization of titania frameworks was possible by rapid thermal treatment at 700 °C, with the retention of the $Im\bar{3}m$ mesostructure after prestabilization of the amorphous networks by heating at a low temperature (300 °C).[12] However, the crystallinity of transition-metal oxide frameworks governs mesostructural stability and it is rational to consider that the mesostructure is sustained by the presence of an amorphous phase that contains semi-crystalline species.[16]

Precise control of mesoscopic structure and crystallinity is crucial for optimization of the photocatalytic performance of titania-based materials; therefore, we investigated the typical photocatalytic degradation of organic molecules over the titania films designed in this study. Photocatalytic performance (550 > 700 > 400 °C) was not proportional to the estimated crystallinity (Figure 2b), which indicates that both the number of active sites (crystallinity) and the porosity of the calcined films are essential for understanding photocatalytic properties. The size and connectivity of mesopores in the calcined films are important for effective diffusion of methylene blue (MB) molecules inside the films.[17,18]

To understand the relationship between the mesostructure and photocatalytic performance of the titania films, we estimate the index for photocatalytic performance of the calcined films by multiplying three index values: crystallinity (see above), effective surface area, and diffusivity. The effective surface area of MB molecules is equivalent to the amount of MB adsorbed on the films at equilibrium. Adsorption of MB molecules was complete within 20 min, and the adsorbed amounts on the films calcined at 400, 550, and 700 °C were estimated to be 0.0166, 0.0112, and 0.0148 mol cm^{-3}, respectively. The other factor, diffusivity of MB, is related to the mesopore size and the porosity (pore volume; 0.34, 0,35, and 0.09 $cm^3 cm^{-1}$), which are estimated from the Kr adsorption–desorption isotherms (Figure 3). Although pore size was not theoretically calculated by using the Kr sorption data, the value of P/P_0 (0.3, 0.5, and 0.8) after complete desorption from the mesopores was normalized on the basis of pore volume and used as the index for diffusivity: 0.102, 0.190, and 0.072 $cm^3 cm^{-3}$ for the films calcined at 400, 550, and 700 °C, respectively. It has also been reported that the pore size of $Im\bar{3}m$ mesoporous titania films becomes large at elevated calcination temperatures.[19] The indexes were calculated by multiplying the three factors to

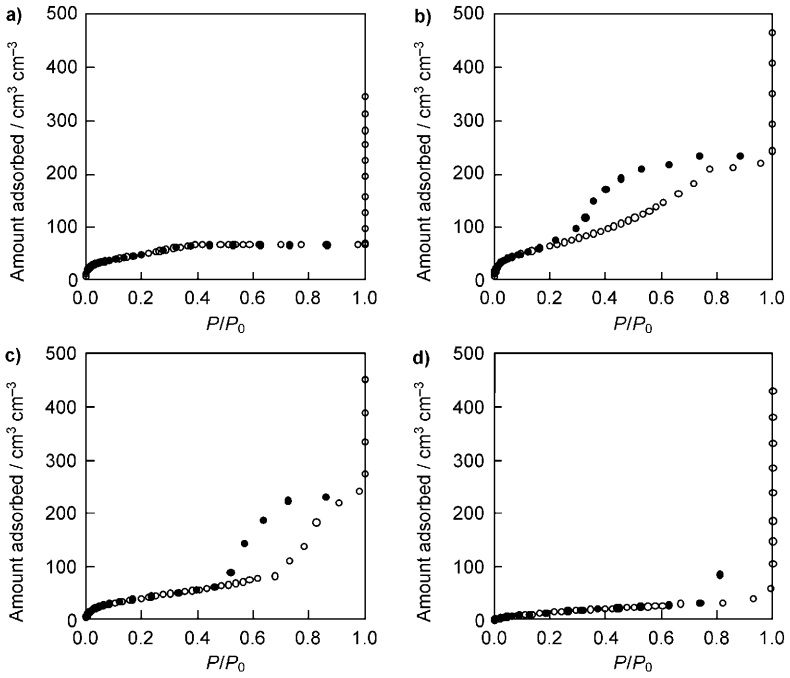

Figure 3. Kr adsorption–desorption isotherms for Pluronic F127-templated titania-based films calcined at a) 250 ($S_{BET}=244\ m^2cm^{-3}$, $V=0.10\ cm^3cm^{-3}$), b) 400 ($S_{BET}=322\ m^2cm^{-3}$, $V=0.34\ cm^3cm^{-3}$), c) 550 ($S_{BET}=194\ m^2cm^{-3}$, $V=0.38\ cm^3cm^{-3}$), and d) 700 °C ($S_{BET}=85\ m^2cm^{-3}$, $V=0.09\ cm^3cm^{-3}$); ○: adsorption, ●: desorption.

give 0.00095, 0.00123, and 0.00106 for the films calcined at 400, 550, and 700 °C, respectively. This is in accordance with the actual photocatalytic performance of the calcined films (550 > 700 > 400 °C).

Titania frameworks in the film calcined at 700 °C were almost completely crystallized to anatase with a size of about 10 to 20 nm. Although the crystallinity (the particle size of anatase nanopillars; ≈10 nm) of the film calcined at 550 °C is lower than that of the film calcined at 700 °C, the photocatalytic performance is higher. Relative porosity related to objective organic molecules should be considered when proposing an appropriate optimal porous structural model with high photocatalytic properties. Indeed, architectural porous films composed of fully crystallized anatase nanoparticles are useful for designing high-performance photocatalysts because the deformation of 3D ordered mesoporous structures leads to the formation of sufficient mesospaces to accommodate target organic molecules.

The importance of the deformation of 3D mesostructures for the improvement of photocatalytic properties will be reported elsewhere, but here we briefly explain the similar deformation of another, 3D hexagonal, mesostructure ($P6_3/mmc$). Because a $P6_3/mmc$ derivative film (thickness 65 nm; S_{BET} 85 m^2cm^{-3}; V 0.04 cm^3cm^{-3}) calcined at 700 °C was also composed of fully crystallized anatase nanoparticles, the photocatalytic properties were simply compared by using two indexes, that is, effective surface area (adsorbed amount of MB) and diffusivity. The effective surface area of the $P6_3/mmc$ derivative film was similarly estimated to be 0.0095 $mol\,cm^{-3}$. The diffusivity in the $P6_3/mmc$ derivative anatase nanocrystal film (5.04, as calculated on the basis of the Kelvin equation, $r \propto -1/\ln(P/P_0=0.82)$, r = radius) was higher than that of the $Im\bar{3}m$ derivative (3.04, $P/P_0=0.72$). Thus, the $P6_3/mmc$ derivative porous anatase nanocrystal film (0.048) was also a promising high-performance photocatalyst similarly to the present cubic ($Im\bar{3}m$) derivative film (0.045) presented herein.

In conclusion, our novel concept based on the poor reactivity of phosphites with transition-metal species for preventing the continuous condensation of metal species in solution can offer the possibility of designed, controlled, and/or predictable synthesis of various advanced metal oxides in the field of sol–gel chemistry. The crystallinity-controlled synthesis of titania was precisely realized in the synthetic system of surfactant-assisted mesoporous inorganic oxides. Condensation-controlled synthesis (related to crystallinity), combined with mesostructural transformation (related to porosity), is applicable to other systems that use transition-metal oxides and are important for the development of porous materials with dramatic performance. Comprehensive rationalization by using actual crystallinity and effective porosity also contributes to the design of porous materials composed of single nanocrystals with both high photocatalytic activity[20] and intelligent electrochemical properties for advanced electrodes in nanodevices.[21,22]

Experimental Section

Condensation-controlled synthesis of mesostructured titania-based material: In a typical synthesis, dehydrated titanium chloride ($TiCl_4$, 0.26 mL; Wako) was slowly added to triethyl phosphite ($P(OC_2H_5)_3$, 0.403 mL, Wako) in ethanol (EtOH, 3 mL; Wako) to give a Ti/P molar ratio of 1.0. After stirring for 10 min, a solution of Pluronic F127 ($EO_{106}PO_{70}EO_{106}$, 0.09 g; Aldrich) in EtOH (3 mL) was added. The mixture was stirred for another 30 min, then the resultant clear solution was spin-coated (3000 rpm) onto quartz substrates to prepare a transparent precursor film with $Im\bar{3}m$ mesostructure, air-dried, and calcined at different temperatures (250–700 °C, 1 °C min^{-1}) for 3 h. The quartz substrates were cleaned by using a UV–ozone treatment (SEN LIGHTS Photo Surface Processor PL16–110) for 15 min before spin-coating.

Fresh $TiCl_4$ was needed for the preparation of highly ordered (cubic $Im\bar{3}m$) mesostructured film because uncontrollable preoligomerization of titanium species that occurs due to the high reactivity of $TiCl_4$ in the presence of moisture was not preferable. In fact, when non-fresh $TiCl_4$

was used for the same synthesis, distinct XRD peaks related to the formation of an ordered mesostructure were not observed (see the Supporting Information, Figure S1). Although designed clusters are very interesting as useful nano building blocks for the direct synthesis of mesostructured materials composed of crystalline units,[23–25] oligomeric titanium species (not structured like clusters) are not suitable as inorganic precursors. This information is useful for the development of reproducible synthetic processes for highly ordered mesostructured materials. Only oligomeric species smaller than ≈ 5 nm in size (smaller than the supposed wall thicknesses) are acceptable for the formation of highly ordered mesostructures.[10]

Photodegradation test by using MB: As described in the literature,[18] photolysis of MB over mesoporous titania films was conducted in a transparent quartz fluorescence spectroscopy cell ($10\times10\times45$ mm^3). The film (on a quartz substrate, $1\times10\times30$ mm^3) was immersed in an aqueous solution of MB (0.01 mM, 3.5 mL). The MB was adequately adsorbed on the entire film after 20 min, then the sample was irradiated from the reverse side of the film in a water bath at 30 °C by using a UV lamp (Ushio, UI501C; Xe). Photodegradation behavior was recorded by using UV/Vis spectroscopy (Shimadzu UV-3100PC) and conversion of MB was calculated from the difference in the absorbance of the peak observed at $\lambda =$ 645–665 nm before and after UV irradiation.

Characterization: GI-SAXS images were obtained by using a Rigaku NANO-Viewer with monochromated $Cu_{K\alpha}$ radiation. TEM images were taken by using JEOL JEM 2010 (200 kV) instrument. A field-emission TEM (JEM-2100F) instrument equipped with an EDX spectroscopy (JED-2300T) instrument was utilized to confirm the composition (Ti/P molar ratio) of the resultant films. Kr adsorption–desorption isotherms were obtained in liquid Ar at 87 K by using a Quantachrome Autosorb-1 instrument. Calcined films on p-type[100] Si wafers with a total area of ≈ 100 cm^2 were introduced in an exclusive sample cell and degassed at RT under vacuum before measurement. Surface area and pore volume were calculated by using the actual area and thickness (verified by using a KLA-Tencor P-15 surface profiler) of the film. XRD patterns were collected at the Kyushu Synchrotron Light Research Center (BL15) by using an 8 keV synchrotron radiation source.

Acknowledgements

This work is partly supported by the Ministry of Economy, Trade and Industry (METI), Japan, as the Environmentally Friendly Sensor Project.

Keywords: crystal engineering · mesoporous materials · photochemistry · porosity · sol–gel processes

[1] A. Vioux, *Chem. Mater.* **1997**, *9*, 2292–2299.
[2] J. N. Hay, H. M. Raval, *Chem. Mater.* **2001**, *13*, 3396–3403.
[3] B. Tian, X. Liu, B. Tu, C. Yu, J. Fan, L. Wang, S. Xie, G. D. Stucky, D. Zhao, *Nat. Mater.* **2003**, *2*, 159–163.
[4] C. Sanchez, J. Livage, M. Henry, F. Babonneau, *J. Non-Cryst. Solids* **1988**, *100*, 65–76.
[5] A. Fujishima, K. Honda, *Nature* **1972**, *238*, 37–38.
[6] A. L. Linsebigler, G. Lu, J. T. Yates, Jr., *Chem. Rev.* **1995**, *95*, 735–758.
[7] B. O'Regan, M. Grätzel, *Nature* **1991**, *353*, 737–739.
[8] U. Bach, D. Lupo, P. Comte, J. E. Moser, F. Weissörtel, J. Salbeck, H. Spreitzer, M. Grätzel, *Nature* **1998**, *395*, 583–585.
[9] M. Grätzel, *Nature* **2001**, *414*, 338–344.
[10] J. Fan, S. W. Boettcher, G. D. Stucky, *Chem. Mater.* **2006**, *18*, 6391–6396.
[11] E. L. Crepaldi, G. J. de A. A. Soler-Illia, D. Grosso, F. Cagnol, F. Ribot, C. Sanchez, *J. Am. Chem. Soc.* **2003**, *125*, 9770–9786.
[12] D. Grosso, G. J. de A. A. Soler-Illia, E. L. Crepaldi, F. Cagnol, C. Sinturel, A. Bourgeois, A. Brunet-Bruneau, H. Amenitsch, P. A. Albouy, C. Sanchez, *Chem. Mater.* **2003**, *15*, 4562–4570.
[13] H. Oveisi, A. Beitollahi, M. Imura, C.-W. Wu, Y. Yamauchi, *Micropor. Mesopor. Mater.* **2010**, *134*, 150–156.
[14] X. Meng, T. Kimura, T. Ohji, K. Kato, *J. Mater. Chem.* **2009**, *19*, 1894–1900.
[15] C.-W. Koh, U.-H. Lee, J.-K. Song, H.-R. Lee, M.-H. Kim, M. Suh, Y.-U. Kwon, *Chem. Asian J.* **2008**, *3*, 862–867.
[16] P. Yang, D. Zhao, D. I. Margolese, B. F. Chmelka, G. D. Stucky, *Nature* **1998**, *396*, 152–155.
[17] M. A. Carreon, S. Y. Choi, M. Mamak, N. Choprab, G. A. Ozin, *J. Mater. Chem.* **2007**, *17*, 82–89.
[18] T. Kimura, N. Miyamoto, X. Meng, T. Ohji, K. Kato, *Chem. Asian J.* **2009**, *4*, 1486–1493.
[19] Y. Sakatani, D. Grosso, L. Nicole, C. Boissière, G. J. de A. A. Soler-Illia, C. Sanchez, *J. Mater. Chem.* **2006**, *16*, 77–82.
[20] G. Liu, C. Sun, H. G. Yang, S. C. Smith, L. Wang, G. Q. Lu, H.-M. Cheng, *Chem. Commun.* **2010**, *46*, 755–757.
[21] L. Grinis, S. Kotlyar, S. Rühle, J. Grinblat, A. Zaban, *Adv. Funct. Mater.* **2010**, *20*, 282–288.
[22] I. Mora-Seró, S. Giménez, F. Fabregat-Santiago, R. Gómez, Q. Shen, T. Toyoda, J. Bisquert, *Acc. Chem. Res.* **2009**, *42*, 1848–1857.
[23] A. Stein, M. Fendorf, T. P. Jarvie, K. T. Mueller, A. J. Benesi, T. E. Mallouk, *Chem. Mater.* **1995**, *7*, 304–313.
[24] C. Sanchez, G. J. de A. A. Soler-Illia, F. Ribot, T. Lalot, C. R. Mayer, V. Cabuil, *Chem. Mater.* **2001**, *13*, 3061–3083.
[25] D. Grosso, C. Boissière, B. Smarsly, T. Brezesinski, N. Pinna, P. A. Albouy, H. Amenitsch, M. Antonietti, C. Sanchez, *Nat. Mater.* **2004**, *3*, 787–792.

Received: May 10, 2010
Published online: September 13, 2010

